Article:
Gorbatenko, I, Bradley, D and Tomlin, AS orcid.org/0000-0001-6621-9492 (2021) Auto-ignition and Detonation of n-butanol and Toluene Reference Fuel Blends (TRF). Combustion and Flame, 229. 111378. ISSN 0010-2180

https://doi.org/10.1016/j.combustflame.2021.02.024

Auto-ignition and Detonation of *n*-butanol and Toluene Reference Fuel Blends (TRF).

Inna Gorbatenko[a,b,c], Derek Bradley,[a] Alison S. Tomlin[b]

[a]School of Mechanical Engineering, University of Leeds, Leeds, LS2 9JT, United Kingdom

[b]School of Chemical and Process Engineering, University of Leeds, Leeds, LS2 9JT, United Kingdom

[c]EPSRC CDT in Fluid Dynamics, University of Leeds, Leeds, LS2 9JT, United Kingdom

Corresponding author: Address: EPSRC CDT in Fluid Dynamics, University of Leeds, Leeds, LS2 9JT, United Kingdom

E-mail: igorbatenko@yahoo.co.uk (I. Gorbatenko)

Abstract

The primary purpose of the paper is to report a study of the auto-ignitive and anti-knock properties, firstly of neat *n*-butanol in air, and secondly of its blends with a gasoline-type, Toluene Reference Fuel (TRF). This involved blending ratios of 10, 20, 40, and 85% of *n*-butanol by volume with a TRF. Pressures were in the range 2-6 MPa, and temperatures ranged from 678 to 916 K. Mathematical modelling of the detailed chemical kinetics for these conditions, using the CANTERA code, yielded values of the duration of the main heat release rate, and revealed the main reactions influencing them. High knock intensities were not anticipated, but checks were made of whether operational points lay within the Detonation Peninsula. This peninsula is

constructed by plotting values of ξ, the ratio of acoustic to auto-ignitive velocity, against ε, the ratio of the transit time of an acoustic wave through a hot spot, to the heat release time (τ_e).

At 2 MPa and 702-855 K, the addition of *n*-butanol to the TRF moved these coordinates away from the peninsula towards the deflagrative regime. At blend ratios of 85%, *n*-butanol mixtures and pure *n*-butanol were found to lie close to the compression curve for methane, known to have good anti-knock properties. This suggests that the addition of *n*-butanol to gasoline would improve knock resistance at this operating condition. However, at 6 MPa and 916 K, the addition of *n*-butanol had the opposite effect, reducing the anti-knock resistance of the blend and pushing it deeper into the peninsula. Uncertainties and limitations of the ξ/ε methodology are also discussed.

Keywords

Detonation peninsula, *n*-butanol blending, auto-ignition, knock, excitation time.

1. Introduction

1.1. *Future Fuels*

An outstanding challenge in terms of achieving pathways to net zero carbon, is the decarbonisation of the transport sector. To promote energy from renewable sources, the Renewable Energy Directive (2018/2001/EU), of the European Union (EU) set a binding target of 32% renewables in its energy mix by 2030, with a sub-target of 14% renewables for road and rail transport [1, 2]. These targets might partially be realised by higher proportions of alternative fuels with petroleum-derived fuels. Current EU legislation limits the proportion of blending ethanol with gasoline to 5%. This proportion is being revised upwards. However, this may not be possible for some older vehicles. In the USA, blends with up to 16% vol butanol in gasoline, are permitted as a legal fuel equivalent of up to 10% vol of ethanol. The lower proportion of oxygen in the butanol molecule gives it a 25% increase in volumetric energy density compared to ethanol [3-5]. This, combined

with the higher stoichiometric air-fuel ratio, enables higher blend ratios of butanol in gasoline of up to 85% [6].

N-butanol offers several advantages over ethanol. The volatility of alcohols decreases with increasing carbon content. As a result, *n*-butanol has a significantly lower vapour pressure than ethanol, minimising evaporation. It has a lower latent heat of vaporisation and a higher flash point than ethanol, facilitating fuel atomisation and combustion during cold start [4]. Furthemore, *n*-butanol is significantly less hygroscopic than ethanol, as well as being less corrosive [3, 4]. This facilitates the use of existing fuel storage, supply and distribution infrastructures.

However, butanol production costs are currently higher than those for ethanol [7] due to the low production yields of butanol in the anaerobic conversion of carbohydrates, with traditional bacterial fermentation to produce acetone, butanol and ethanol (ABE). The theoretical butanol yield is about 20% less than that of ethanol, while its energy value (68 MJ/Gasoline Gallon Equivalent (GGE)) is approximately 33% higher than that of ethanol (51 MJ/GGE) [8]. Lower costs or higher yields could make *n*-butanol a more viable competitor to ethanol, that could potentially be blended to higher ratios with gasoline, without significant engine modifications.

1.2. ***Engine Knock Parameters***.

The power of spark ignition (SI) engines is limited by the onset of knock. This aspect has been well-reviewed, by Kalghatgi [9] and Wang et al. [10]. The Octane Numbers (ONs), introduced in 1927, are used to describe the gasoline fuel knock propensity. ON is defined by comparison with the mixture of the two Primary Reference Fuels (PRF), *iso*-octane and *n*-heptane, which have the same anti-knocking capacity as the fuel under test. However, together, *iso*-octane and *n*-heptane

comprise no more than about 6% by mass of most gasolines. The associated Research and Motor Octane Numbers, RON and MON, are measured under standardised engine test conditions, with inlet temperatures of 325 K and 422 K, respectively. However, engine turbo-charging and the development of more knock-resistant fuels have resulted in increased operational pressures, power outputs, and efficiencies, when compared with older engines.

To provide a broader fuel characterisation than that of the ONs, Octane Indices, OI, have been evaluated. For given running conditions, the OI is the octane number of the PRF that just knocks under the same conditions as the chosen gasoline. It is sufficiently accurate to equate the delay time of the non-PRF to that of the corresponding PRF under the same conditions for 10% heat release. It is found that the auto-ignition delay times, τ_i, of the non-PRF fuels can be higher than those of the associated RON. This is most marked with olefenic and toluenic fuels [11]. Clearly, in this situation, the ON is no longer an adequate, universal, parameter.

With aromatic contents in current diesel and gasoline fuels of between about 25 and 35%, the associated superior anti-knock properties, require more detailed assessment. When gasolines have higher values of τ_i than is suggested by their RONs, different comparators are required. Toluene Reference Fuels, TRF, comprised of *n*-heptane, *iso*-octane and toluene, add an aromatic compound to the conventional primary reference fuels, and can have higher τ_i values for the same RON. Such mixtures can potentially provide a better representation of ignition delay properties than those based on a binary mixture. Consequently, following Agbro et al. [12], a TRF of mole fractional composition 0.114 *n*-heptane, 0.6564 *i*-octane, and 0.2297 toluene was used as a surrogate for RON 95, MON 86.6 gasoline in the present study.

An alternative to measuring the knocking tendency of a fuel in terms of that of standardised fuel blends, is to express it, more directly, in terms of values of its primary auto-ignition parameters. This is the methodology of the parametric ξ/ε, detonation peninsula approach [13]. In it, the key parameters are the auto-ignition delay time, τ_i, and the duration of the associated main heat release rate, τ_e. When appropriately incorporated with values of engine pressures and temperatures, the boundaries within which engine knock becomes probable are defined. This regime forms a peninsula, that is rather similar for most fuels [14]. Engine studies have shown this approach, over a range of temperatures and pressures, to define the onset of mild and strong knock successfully for a number of fuels, under a variety of operational conditions. Within the boundaries of the developing detonation peninsula, knock of different intensities might occur. The coordinates for these bounds are expressed in terms of auto-ignition at an igniting hot spot of radius r_o, the ratio of acoustic to auto-ignitive velocity (a/u_a), and the ratio of the acoustic wave residence time in the hot spot, r_o/a, to the duration of the heat release rate, τ_e.

1.3. *Aims and Summary of the Paper*

Although *n*-butanol has a higher energy density than ethanol, it has a lower octane rating and the potential octane enhancing benefits of *n*-butanol addition are unclear. The aim of this study was to employ the detonation peninsula approach to improve understanding of the effects of the addition of *n*-butanol, to a gasoline-type fuel, on the knocking tendency of the resulting blend. However, it was observed that in the RCM measurements of τ_i for gasoline-type fuels, there were variations in the ensuing onset of auto-ignitions. An unambiguous rapid uniform pressure rise is indicative of uniform auto-ignition. A slower, less uniform, pressure rise can be indicative of multiple auto-ignitions, possibly combined with a degree of deflagrative burning from a hot spot. This might be

confirmed by the detonation peninsula. This prompted a study of modes of ignition, where both prompt uniform auto-ignition can occur, as well as non-uniform auto-ignition, arising from mixture/temperature heterogeneities [15-17]. Hence, a secondary aim of the work is to explore whether an RCM is an appropriate facility for ignition delay studies of gasoline-type fuels and their blends. Furthermore, with brute force sensitivity analysis, for the first time, the chemistry controlling the τ_e value of the *n*-butanol/TRF blends was investigated to determine the main reactions which influence τ_e, at selected conditions and blending ratios.

The paper first summarises the bounds of the detonation peninsula, and shows how these can predict the onset of auto-ignition and the development of knock. It then presents τ_i and novel τ_e data for *n*-butanol, TRF, and their blends. These are used to derive values of ξ and ε. Where these lie, in relation to the boundaries in the diagram, determines the propensity of the fuel to knock. The fixed boundary of the ξ/ε detonation peninsula defines the onset and development of knock over different ranges of temperature and pressure. Other regimes are defined outside the peninsula. The blends are referred to as B10, B20, B40, and B85, where B10 indicates 10% by volume of *n*-butanol in a mixture with the TRF. Initially, data are generated for *n*-butanol, and all mixtures, at 2 MPa and 678-916 K, in line with available ignition delay data. Additional modelling at more severe thermodynamic conditions of 745-916 K and 4-6 MPa is also performed, to assess further the effects of *n*-butanol addition on the blend's tendency to detonate, within the ξ/ε framework. Finally, the limitations and uncertainties of the ξ/ε methodology are discussed.

2. Methodology

2.1. *Detonation Peninsula*

The auto-ignitive velocity, u_a, at a spherical hot spot radius, r, is $\delta r/\delta\tau_i$, with E/R the activation temperature of the auto-ignition delay time, τ_i. This leads to the relationship [18, 19]:

$$\xi = \frac{a}{u_a} = a\left(\frac{\delta T}{\delta r}\right)\left(\frac{\delta \tau_i}{\delta T}\right) = \tau_i\left(\frac{E}{RT^2}\right)\left(\frac{\delta T}{\delta r}\right)a \qquad (1)$$

ε is the residence time, r_o/a, of the developing acoustic wave within the hot spot of initial radius, r_o, normalised by the temporal duration of the heat release, namely the excitation time, τ_e [13]:

$$\varepsilon = \frac{r_0}{a\tau_e} \qquad (2)$$

The higher the value of ε, the greater the reinforcement of any potential acoustic wave initiated by the heat release and the extent of any detonation. The higher the value of ξ, the more deflagrative is the ensuing propagation front, after a hot spot auto-ignition. Although, further auto-ignitions are possible at higher ξ values, the resulting pressure pulses would be relatively weak, with no transition to detonation [14]. A detonation peninsula, and neighbouring combustion regimes [14], are shown in Fig. 1.

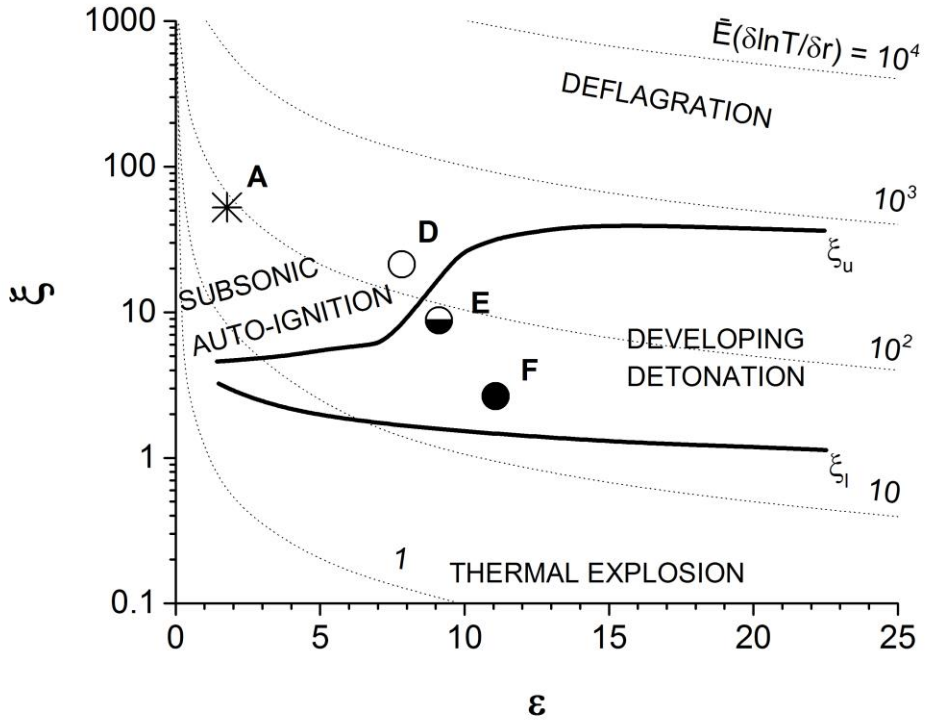

Figure 1: Regime diagram for hot spot auto-ignition. Increasing black fill of the circle symbol indicates increasing severity of knock. Conditions D, E, and F are for a stoichiometric RON 95/ MON 85, OI = 105 (0.62 *iso*-octane, 0.29, toluene, 0.09 *n*-heptane), at 800 K and 7 MPa, 850 K and 9 MPa, and 926 K and 12.8 MPa, respectively. Condition A is for lean-burning benign auto-ignition of PRF84 at φ=0.25, 729 K and 6.52 MPa. Adapted from Bates et al. [14].

Within the literature, data for the construction of the ξ/ε peninsula were derived originally from numerous direct numerical simulations of the auto-ignition of H_2/CO/air mixtures at spherical hot spots, under a variety of conditions [13]. Subsequently, Peters et al. [20] demonstrated the peninsula boundaries to be equally valid for hydrocarbons [14]. Pan et al. [21] also have provided additional chemical kinetic confirmation of the boundaries of the ξ/ε detonation peninsula through their numerical simulations, involving CH_4, CH_3OH and H_2. These simulations confirmed that,

below the lower branch of the peninsula, the speed of the reaction wave was much higher than that of the Chapman Jouget propagation speed. Above the upper branch, all propagation speeds were subsonic. Close to the upper branch, H_2 had the lowest hot spot sizes, a consequence of its smallest τ_e. CH_4 and CH_3OH had larger τ_e, and higher r_0, that increased with ε. Outside the developing detonation peninsula are regimes of deflagration and subsonic auto-ignitive propagation. Inside the peninsula the black circle indicates coordinates of super knock [13].

It was shown in Bates et al. [14] that:

$$\xi\varepsilon = -\bar{\mathrm{E}}\left(\frac{\delta \ln T}{\delta \bar{r}}\right), \text{ where } \bar{r} = r/r_0 \text{ and } \bar{\mathrm{E}} = \frac{\tau_i}{\tau_e}\frac{E}{RT}, \tag{3}$$

and that the benign auto-ignitive regime becomes much more conventionally deflagrative when $\bar{E}\partial \ln T/\partial \bar{r} > 1500$. Below about $\xi = 1.0$ is the regime of thermal explosion.

The detonation peninsula has proved to be practically useful in several contexts, including the general hazard assessment of flammable mixtures. Solutions of mathematical models of the turbulent flow and flame propagation in engines, can be post-processed, using the ξ/ε diagram to indicate the propensity for an engine to knock and its severity [22]. Advancing the spark timing of engine ignition has been shown to increase the proportion of engine cycles entering the detonation peninsula [23]. Regimes have been usefully identified in RCMs [24]. In the present study, it is assumed that the temperature gradient is -2 K/mm, based on engine and other measurements [14]. A hot spot radius, r_0, of 5 mm was assumed, which was also chosen by Kalghatgi et al. [25] and Rudloff et al. [26].

2.2. *Ignition Delay and Excitation Times*

ξ values were calculated, from the activation temperature of the auto-ignition delay times obtained from the RCM measurements of Gorbatenko et al. [27] for B10, B40 and B85 blends, as well as for the pure TRF, B20, and pure *n*-butanol of Agbro et al. [12]. Here, B10 indicates 10% by volume of *n*-butanol in a mixture with the TRF. Calculations of ε involved detailed chemical kinetic modelling of τ_e.

The CANTERA [28] package was used to simulate τ_e using a variable volume approach, with imposed effective volume histories to account for the effects of heat loss to the chamber walls and heat release during piston compression in experiments. Using the isentropic law, effective volume histories were derived from representative non-reactive pressure profiles, where in the experiments O_2 was replaced with N_2. The volume histories were adopted from Gorbatenko et al. [27] and were employed as inputs in the CANTERA simulations. The same technique is commonly applied in simulations of τ_i under RCM conditions. Simulations employed a reduced combined mechanism for *n*-butanol, from Sarathy et al [29], and for the TRF surrogate, from Mehl et al. [30], modified with the suggestions in Agbro et al. [31]. This kinetic scheme is provided as Supplementary Material in Gorbatenko et al. [27]. Following Lutz et al. [32], τ_e was defined as the time from the point where the heat release rate was 5% of the maximum heat release rate to the instant at which that maximum value was achieved.

For each value of ξ, values of acoustic speed, a, for every fuel blend and studied, conditions were calculated using the CANTERA package.

2.3. *Sensitivity Analysis*

In order to determine the principal reactions that affect τ_e, brute force local sensitivity analyses were employed, using τ_e as the target output for all fuel blends tested at $\varphi = 1$, $P = 2$ MPa, and various temperatures. All used constant volume simulations. The A-factors of all reactions were increased sequentially by 10% from their nominal values, while all other parameters retained their base values. The influences of A-factor increase on reaction excitation times were calculated by performing a new simulation for each parametric change. The excitation time sensitivity for each reaction i in the mechanism was estimated as:

$$S_i = \left(\frac{\tau_0 - \tau_1}{\tau_0}\right), \quad (4)$$

where S_i is the sensitivity coefficient of reaction i, τ_0 is the excitation time computed with the original kinetic scheme, without any changes to A-factors, and τ_1 is the excitation time modelled when one of the reaction rates has been perturbed. Consequently, a positive sensitivity index represents a decrease in the magnitude of τ_e, while a negative sensitivity index results in increased values of τ_e. The S_i values for each blend were normalised by the maximum sensitivity at each temperature. Hence, the reaction with the highest effect on the predicted τ_e has a sensitivity index of 1.

3. Excitation Times.

The earlier experimental values τ_i of Gorbatenko et al. [27] and the modelled values of τ_e for stoichiometric air mixtures of *n*-butanol, TRF, with their blends, between 678 and 916 K, at 2 MPa, are shown in Figs. 2 and 3, respectively. As highlighted by Gorbatenko et al. [27], ignition delays for pure *n*-butanol exhibit a more Arrhenius-like temperature dependence, while pure TRF

exhibits a pronounced Negative Temperature Coefficient (NTC) regime. At low temperatures, the addition of *n*-butanol suppresses reactivity, increasing ignition delays. At higher temperatures, this trend is reversed. These effects of *n*-butanol addition to the TRF affect the magnitude of the resulting ξ value, and, hence, the location of the blends on the ξ/ε diagram.

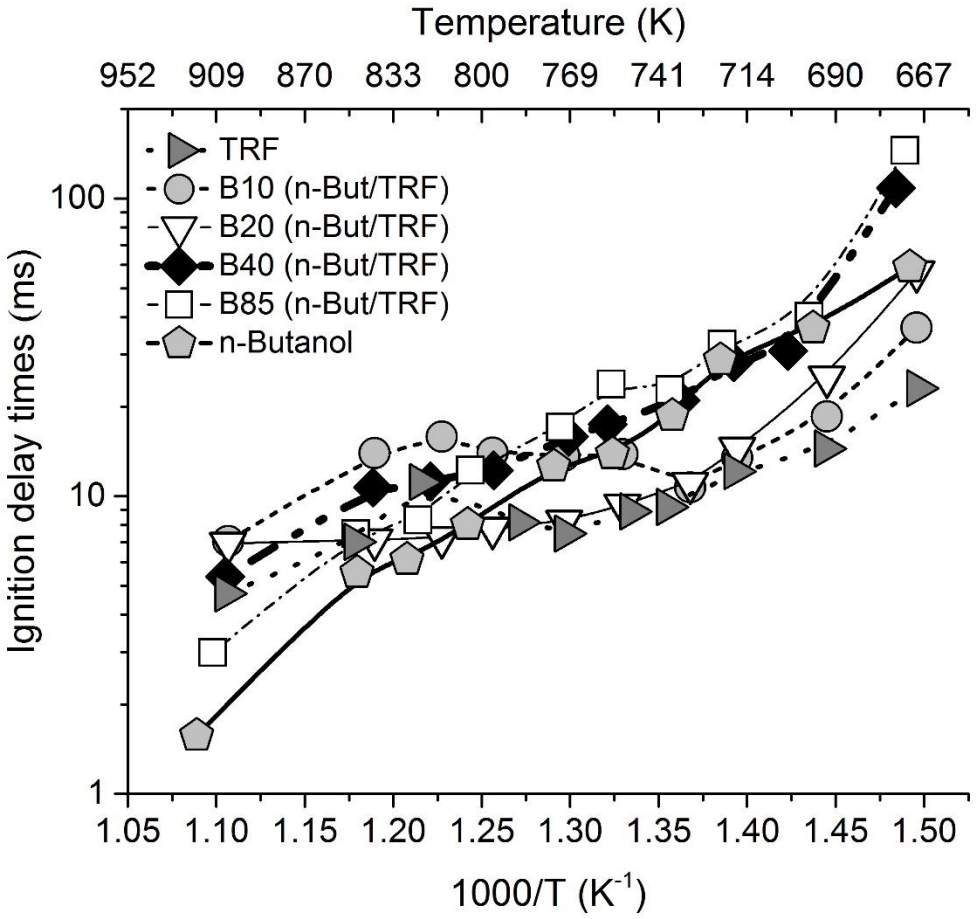

Figure 2. Experimentally measured ignition delay times of *n*-butanol, TRF, and their blends with air, under stoichiometric conditions at 2 MPa and 678-916 K, within an RCM. Adapted from Gorbatenko et al. [27].

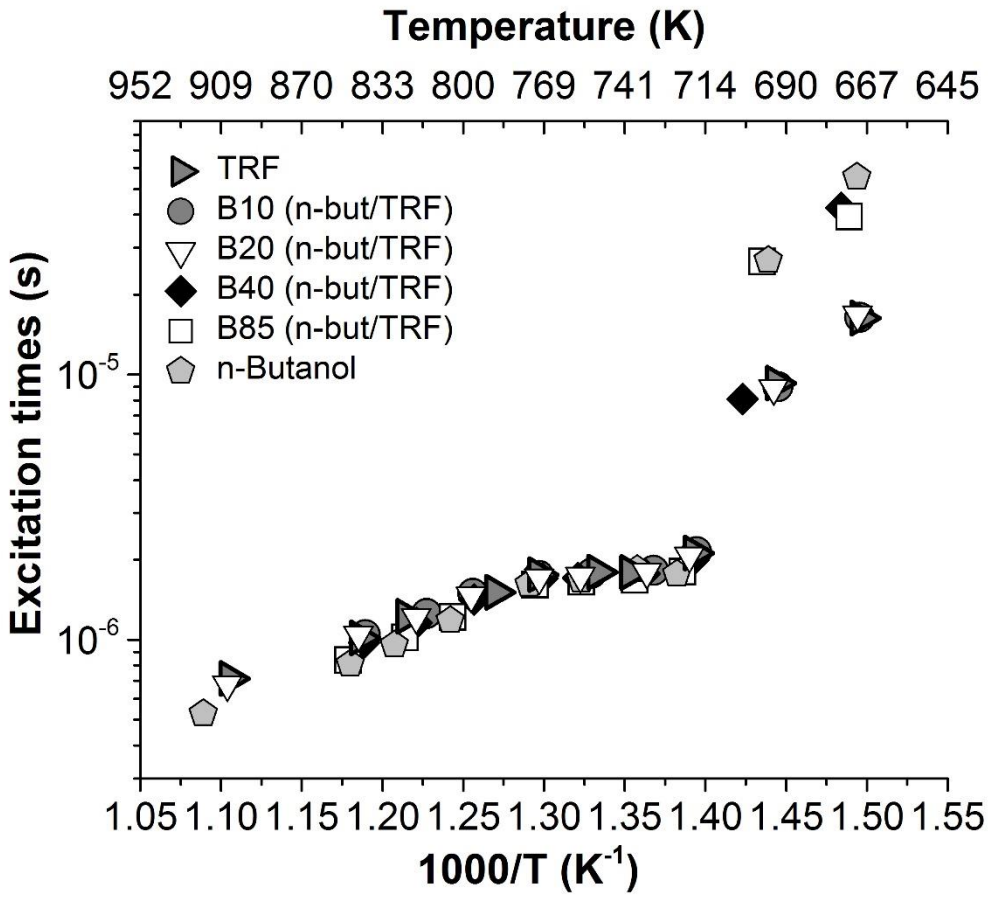

Figure 3. Modelled excitation times of *n*-butanol, TRF, and their blends with air, under stoichiometric conditions at 2 MPa and 678 - 916 K.

There are two striking characteristics of Fig. 3. First, a low temperature regime exists, in which τ_e falls sharply with increasing *T*. This is followed by a higher temperature regime, with lower τ_e values. These fall less sharply with increasing *T*, and are independent of the fuel blend. The maximum value of τ_e at the start of this higher temperature regime is 2.14 x 10^{-6} seconds. With r_0= 5 mm, this gives ε= 4.51, a value that increases with temperature. The results suggest that in the high to intermediate temperature range, the τ_e values lie on a single curve for the various fuels. Contrary to the response of ignition delay times in Fig. 2, there is no apparent effect of *n*-butanol

addition to the TRF blends, nor any obvious influence from NTC chemistry on τ_e. The excitation times show an almost logarithmic increase with temperature. The main contributing reactions are discussed further in the section on sensitivity analysis.

At lower temperatures, the τ_e values of the B10 and B20 blends are comparable to those of the pure TRF mixture. The behaviour of the higher blend of B85 is similar to that of pure *n*-butanol. Here, the higher *n*-butanol blends also have larger τ_i values, compared to the lower *n*-butanol blends. Hence, the low temperature heat release is likely to have some indirect impact on the magnitude of τ_e, causing the scatter at low temperatures. This implies that the fuel composition becomes important only at low temperatures, and τ_e is not fuel-specific at higher temperatures. This peculiar behaviour of excitation times is explored by sensitivity analyses later in this section. Note, it is not possible, on the requisite order of microseconds, to measure τ_e. Values of τ_e are based entirely on the detailed chemical kinetic scheme.

Conversely, as mixtures become less reactive through temperature reduction, or dilution with inert gas, the mixture moves into a regime of sharply increasing τ_e. This effect has been well illustrated by Dai et al. [33]. Reactivity was reduced by the addition of CO_2 to stoichiometric *n*-heptane/air at 100 K and 4 MPa. With r_0 = 5 mm, an added molar fraction of 0.21 CO_2 gave a minimal value of ε of 3.5.

Because all fuels decompose to basically the same set of small C_1-C_3 hydrocarbons, high temperature auto-ignition processes are rather insensitive to fuel structure [34]. These smaller hydrocarbons oxidise to yield CO and CO_2. In all cases the high temperature combustion chemistry is dominated by small molecule, hydrogen-related, CO-to-CO_2 chemistry. Different fuel blends

follow similar high temperature chemistry pathways, as will be demonstrated by the sensitivity analysis. Clearly, a lack of fuel specificity in the τ_e chemistry is to be expected [34].

Figure 4 shows the normalised sensitivity indices for excitation times for *n*-butanol, TRF, and all blends at 678, 765, 916 K and 2 MPa, under stoichiometric conditions. It shows the 6 most influential reaction sensitivities at each of the three temperatures. These reactions are listed in Table 1, with their heats of formation. Despite different reaction conditions, the reactions of hydrogen, carbon monoxide and the smaller C_1 molecule chemistry dominate sensitivities and primarily control τ_e. This highlights the characteristics of high temperature chemistry for the hydrocarbon fuels. Despite some small differences between the blends for τ_e at low temperatures, individual fuel specific reactions are not highly ranked in the sensitivity analysis, and hence do not feature in the figure.

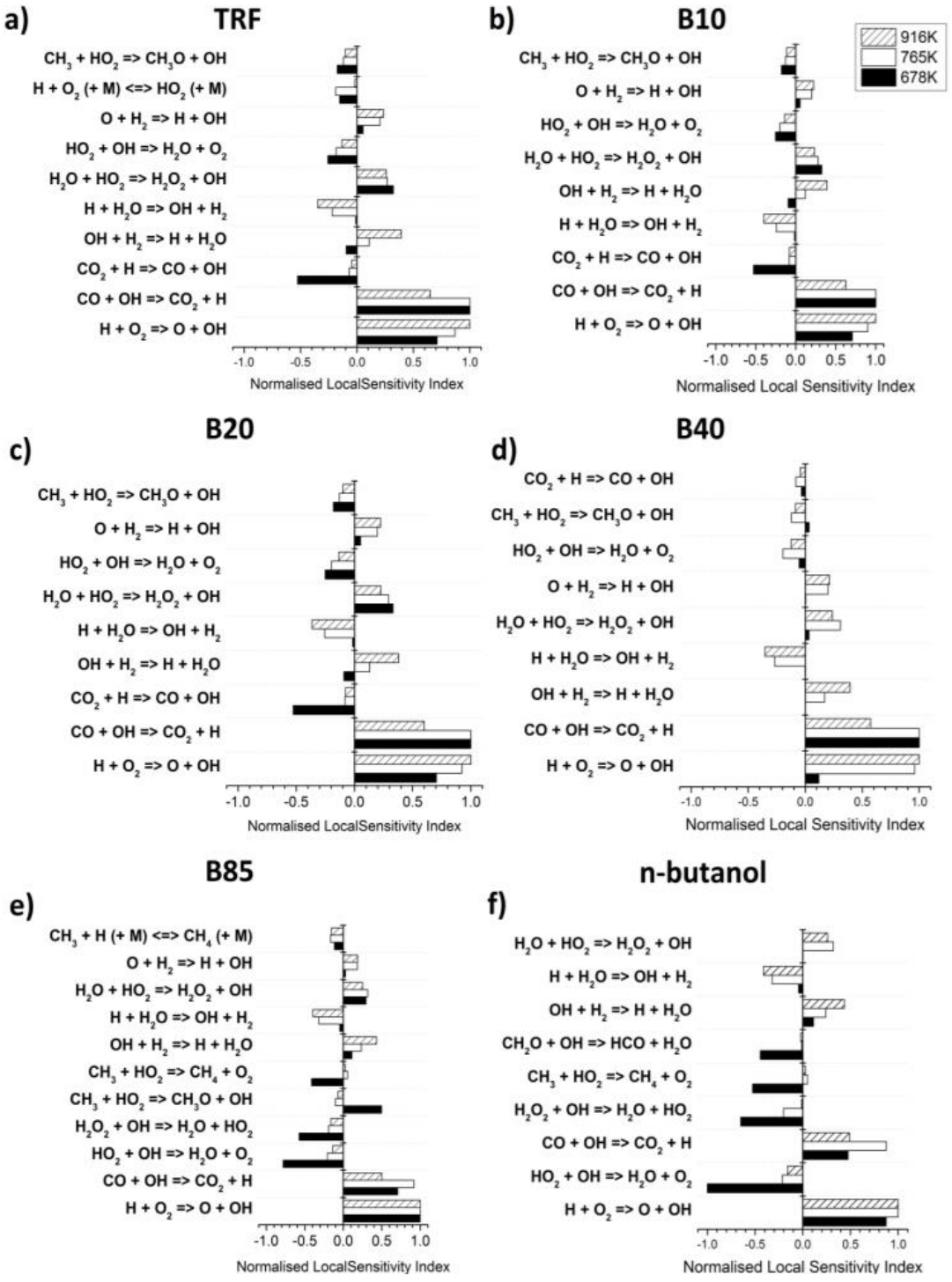

Figure 4. Normalised brute force local sensitivity indices for τ_e stoichiometric mixtures at 678, 765, and 916 K, and 2 MPa.

Table 1. Principal reactions highlighted by sensitivity analysis for τ_e stoichiometric mixtures and their associated enthalpies (kJ/mol) at P=2 MPa and 678, 765 and 916 K. A positive enthalpy change represents an endothermic reaction, and a negative one, heat-releasing exothermic processes.

Reaction	**The enthalpy (kJ/mol) for the reaction at P=2 MPa and T**		
	678 K	**765 K**	**916 K**
$H+O_2 \rightarrow O+OH$	68.11	67.85	67.31
$H+H_2O \rightarrow OH+H_2$	62.14	62.23	62.23
$H+O_2(+M) \leftrightarrow HO_2(+M)$	-210.20	-211.07	-212.47
$O+H_2 \rightarrow H+OH$	5.93	5.94	6.00
$OH+H_2 \rightarrow H+H_2O$	-62.14	-62.23	-62.23
$HO_2+OH \rightarrow H_2O+O_2$	-292.59	-292.86	-293.26
$H_2O+HO_2 \rightarrow H_2O_2+OH$	132.69	133.25	134.18
$H_2O_2+OH \rightarrow H_2O+HO_2$	-132.69	-133.25	-134.18
$CO+OH \rightarrow CO_2+H$	-100.21	-99.38	-97.79
$CO_2+H \rightarrow CO+OH$	100.21	99.38	97.79
$CH_2O+OH \rightarrow HCO+H_2O$	-126.51	-126.63	-126.96
$CH_3+HO_2 \rightarrow CH_3O+OH$	-105.38	-105.40	-105.27
$CH_3+HO_2 \rightarrow CH_4+O_2$	-235.76	-235.99	-235.96
$CH_3+H(+M) \leftrightarrow CH_4(+M)$	-445.96	-447.06	-448.43

The definition of τ_e is governed by the high temperature heat release around the time of the main ignition. However, low and intermediate temperature heat release are also apparent in a multi-stage ignition of larger hydrocarbon fuels, such as *n*-butanol/TRF blends at low temperatures [35-37]. Early stage heat release is generally characterised by low temperature chemistry and is related to the presence of an NTC, displayed in Fig. 2. The low temperature heat release raises the temperature of the system and establishes a radical pool. This can substantially accelerate the main

ignition, and influence the magnitude of τ_i. On the other hand, pure *n*-butanol exhibits single-stage auto-ignition behaviour. Its addition to a TRF supresses the low temperature heat release and, consequently, the reactivity of the system leading to longer ignition delay times, as demonstrated in Fig. 2. H-abstraction by OH from the α-carbon site ($nC_4H_9OH + OH \leftrightarrow C_4H_8OH\text{-}1 + H_2O$) is the most sensitive reaction at low and intermediate temperatures for high *n*-butanol/TRF blends, as shown in the ignition delay studies of Gorbatenko et al. [27]. This reaction has an inhibiting role, slowing down the reactivity of the system, due to the successive O_2 addition to α radicals, leading to the formation of an aldehyde and HO_2 (a less reactive radical than OH at low temperatures) via direct elimination. For the low *n*-butanol/TRF blends, it competes with chain branching reactions from the surrogate gasoline, as shown in [27], specifically the H abstraction reactions from *n*-heptane, and from the primary and secondary sites of *iso*-octane. These competing chain branching reactions reduce τ_i at lower temperatures, increasing the depth of the NTC, as the *n*-butanol concentration is reduced.

The smaller NTC and longer ignition delays at low temperatures for higher *n*-butanol blends are related to this increased importance of HO_2 chemistry. The addition of *n*-butanol, increases the amount of HO_2 due to the importance of H abstraction from the α-site of *n*-butanol. This is followed by the subsequent direct elimination of HO_2, which is considerably less reactive than OH. At high blends, HO_2 can survive until the main stage of ignition, which is also associated with a smooth and relatively slow growth in pressure of the non-knocking combustion [15, 16]. Through the ignition the HO_2 is rapidly consumed, forming H_2O_2. This either decomposes to form two OH, promoting reactivity, or reacts with OH to form water and HO_2 which reduces reactivity. Figure 4 clearly shows the increased importance of $H_2O_2 + OH \rightarrow H_2O + HO_2$ on τ_e for higher *n*-butanol blends. Substantial exothermicity is associated with propagation of the OH radical, while HO_2

propagation, leading to H_2O_2 formation, is virtually thermo-neutral [38]. Hence, the overall heat release rate is reduced for higher *n*-butanol blends at low temperatures, resulting in a longer τ_e , as illustrated in Fig. 3. In addition, for B85 and pure *n*-butanol, HO_2 can consume OH via $HO_2 + OH \rightarrow H_2O + O_2$, which is an exothermic termination reaction leading to an increase in τ_e. Hence, although there are no fuel specific reactions amongst those highly ranked in the sensitivity analysis, the fuel specific chemistry has an influence on the radical pool, with the importance of $HO_2 + OH \rightarrow H_2O + O_2$ increasing, with an increase in the *n*-butanol content within the blend.

For pure TRF and the lower *n*-butanol/TRF blends the OH consuming reaction, $CO + OH \rightarrow CO_2 + H$, is dominant at low and intermediate temperatures, with an increase in its A-factor, resulting in a positive sensitivity index and a decrease in τ_e. This reaction is a major heat generating reaction, and is very important for all fuels across all temperatures. A reason for this is that when the final CO oxidation occurs (around the time of the high temperature heat release governing τ_e), the composition of the charge is very similar, regardless of the structure of the original fuel molecule. Its endothermic reverse reaction, $CO_2 + H \rightarrow CO + OH$, is the main opposition to this reaction for pure TRF, and the lower *n*-butanol/TRF blends. The chain termination reaction $CH_3 + HO_2 \rightarrow CH_4 + O_2$, displays a negative sensitivity index and is important for B85 and pure *n*-butanol. An alternative channel is the major chain branching reaction $CH_3 + HO_2 \rightarrow CH_3O + OH$. This is an important reaction for HO_2 consumption. It is highlighted in the sensitivity analyses for all fuels. In addition, the resulting methoxy radicals (CH_3O) are unstable and readily decompose, to form H and CH_2O.

At high temperatures, the endothermic $H + O_2 \rightarrow O + OH$ dominates the sensitivity analysis for τ_e, supporting its increasing dominance with temperature increase. This promotes chain branching

processes. A positive sensitivity index indicates that an increase in its reaction rate leads to a decrease in τ_e magnitude. For the pure TRF, H + O_2 → O + OH competes with H + O_2(+M) ↔ HO_2(+M), with the former linked to the development of knock [15, 16]. Also, OH + H_2 → H + H_2O competes with H + H_2O → OH + H_2. These reactions are extremely important in the oxidation of all fuels at high temperatures.

4. The ξ-ε Diagram

Figure 5 shows ξ and ε values at 2 MPa for stoichiometric mixtures of the different blends and *n*-butanol, and the Detonation Peninsula. Temperatures, all less than 855 K, are given in the caption. Auto-ignition parameters for these fuels are provided as supplementary material in TableS1. The figure also shows plots for stoichiometric mixtures of CH_4 and PRF 98 from Bates et al. [18].

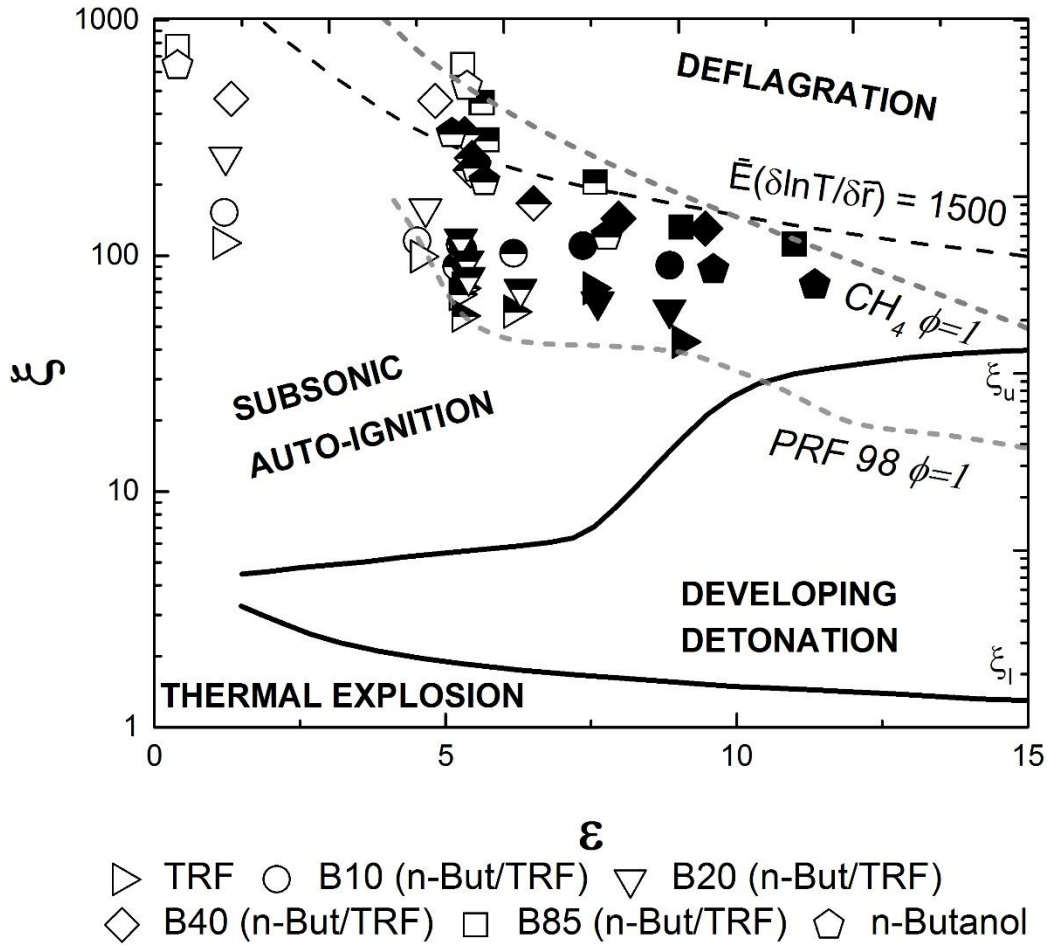

Figure 5. Comparisons of ξ against ε values for stoichiometric *n*-butanol/TRF blends with stoichiometric CH_4 and PRF 98 from Bates et al. (dashed lines) [18]. Symbols: Open 702-727 K, half open 727-831 K, filled 831-855K.

Pure *n*-butanol, TRF fuel and their blends lie outside the detonation development region, and the peninsula. Mixtures closest to the peninsula are those of methane, TRF, and *n*-butanol, at 855 K. B85 appears to be the most resistant to detonation, lying close to the compression curve of methane, known to have good anti-knock properties. The PRF 98, φ=1, entered the detonation peninsula at a pressure of 6.5 MPa and 925 K [18]: a significantly more reactive mixture than the others, and the only one to enter the peninsula. Its thermodynamic conditions of 6.5 MPa and 925

K are significantly higher compared to those studied here of 2 MPa and 702-855 K. The effects of increasing the severity of operating conditions on the likelihood of *n*-butanol/TRF blends detonating are investigated in Section 6.

Low temperature heat release and multi-stage ignition behaviour significantly alter the auto-ignition behaviour of the fuel blend. They raise the local temperature and lead to locally lower temperature gradients that might cause supersonic auto-ignition waves, hence rapid ignition. Changes in temperature gradients of hot spots affect the mode of the auto-ignition. Their increase leads to more enhanced coupling between chemical and pressure waves, promoting detonation development. TRF, B10, and B20 fuels displayed an NTC behaviour, as discussed in Section 3. ξ values of these fuels are seen to almost systematically reduce with an increase in temperature in the temperature range between 727 and 782 K. However, they are seen to increase with a further rise in the initial temperature, whereas for B85 and pure n-butanol, ξ values are seen almost always decrease with an increase in temperature. Also, B40 and B85 display higher ξ values than pure *n*-butanol. Hence, an addition of *n*-butanol attenuates the NTC chemistry, that in fact alters the detonation tendencies of the resultant blend.

5. Auto-ignition/Deflagration Transition

Ignition at a hot spot can provide the onset of general auto-ignition of the entire mixture, or be the first-stage of either an auto-ignitively propagating flame, or of a normal turbulent flame deflagration [17]. A tentative threshold for the onset of turbulent deflagration is [14]:

$$\xi\varepsilon = \bar{\mathrm{E}}\left(\frac{\delta lnT}{\delta \bar{r}}\right) = 1500, \tag{5}$$

represented by a dashed curve in Fig. 5. Auto-ignitive propagation could occur in the regime marked *subsonic auto-ignition* in Fig. 5 [14, 18, 39].

Because of uncertainties in hot spot sizes and temperatures, there cannot be a well-defined boundary between auto-ignitive and deflagrative regimes. Ideally, in RCMs, measurements of τ_i would occur with spatially uniform mixtures, at constant temperature. However, if the mixture is not uniform, auto-ignition will first occur at the most reactive hot spot, from which reaction might propagate autoignitively, or in a deflagrative mode. Such variable delay times would impair both repeatability and accuracy.

Low values of $\bar{E}(\delta lnT/\delta\bar{r})$ are associated with the more stable and repeatable auto-ignitions in RCMs, and with knocking combustion in spark ignition (SI) engines. Hence, SI engines, in contrast to RCMs should avoid low values of $\bar{E}(\delta lnT/\delta\bar{r})$. A variety of such values, evaluated from Eq. (3) for a range of fuels, are plotted against the charge mean temperature in Fig. 6. This includes a shaded transition zone for values of $\bar{E}(\delta lnT/\delta\bar{r})$, extending from 750 to 7,000.

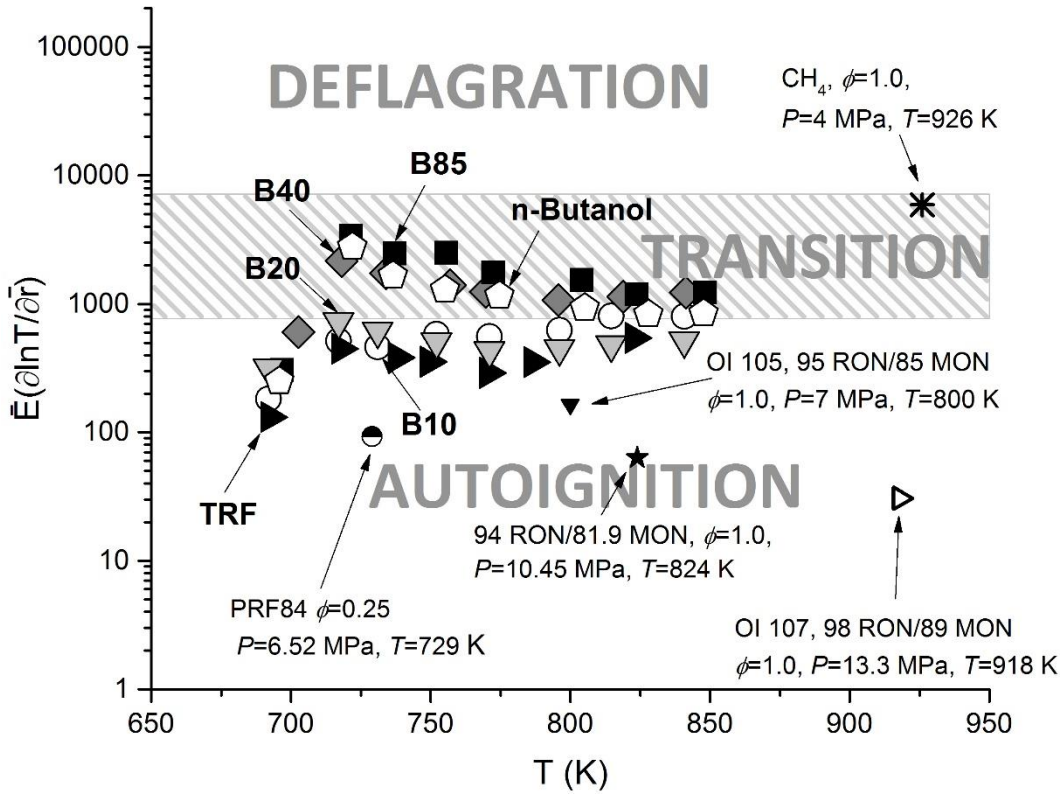

Figure 6. Values of $\bar{E}(\delta lnT/\delta\bar{r})$ as a function of *T,* for stoichiometric TRF, *n*-butanol, B10, B20, B40 and B85 *n*-butanol/TRF blends, as well as engine operational data for other fuels from Bates et al. [39] and Bates et al. [18]. Three reaction regimes can be discerned: flame front deflagration, auto-ignition and auto-ignitive deflagration in a transition regime.

In this figure, the lowest values of $\bar{E}(\delta lnT/\delta\bar{r})$ occur with the TRF, B10, and B20 blends, which are clearly in the auto-ignition regime, as is also shown in Fig. 5. At high temperatures, the measurements in Fig. 2 exhibited a classical, constant pressure record, followed by a rapid pressure rise. At lower and intermediate temperatures, B85 and B40 show more gradual pressure rises, with an increasing radius of curvature on the pressure record as the pressure begins to rise. This is indicative of a less spontaneous uniform auto-ignition. These two blends have the highest values

of $\bar{E}(\delta lnT/\delta\bar{r})$, which are in the transition regime, but closest to that of turbulent deflagration, with the highest values of ξ in Fig. 5.

Overall, the results presented in Figs. 5-6 suggest that the RCM is operating predominantly in the auto-ignitive regime, with some excursions into the transition regime, but with no deflagrative influence. Non-uniform, transitional, auto-ignition is usually more commonly observed in the NTC region [40]. The fuels with apparent NTC auto-ignition behaviour, namely pure TRF and the lower *n*-butanol/TRF blends, were found to lie below the suggested mixed deflagration/auto-ignition transition regime. It is concluded that ignition delay measurements in RCMs can be reliable targets for the validation of chemical kinetic models of gasoline-type fuels, but there must be awareness of the proximity of the deflagrative regime.

Figure 5 demonstrates that the low temperature chemistry in the cases of cold spots and the NTC region for pure TRF and low *n*-butanol/TRF blends have little effect on detonation development in the peninsula, due to the low auto-ignitive velocities, and higher values of ξ. This could be attributed to the reaction front being primarily driven by high temperature heat release, while that at low temperature has a secondary effect on chemical-acoustic interactions. In contrast, the low temperature heat release behaviour has a significant effect on the knocking intensity. Moreover, it is worth noting that both ξ and ε contain inherent uncertainties as discussed in Section 7.

6. Effects of *n*-butanol Addition at High Pressure

The data in Figs. 5 and 6 suggest *n*-butanol, and particularly its high level blends with TRF, might have good knock resistance. However, the question arises as to the conditions that would cause the entry of such blends into the detonation peninsula. Consequently, constant volume simulations

of τ_i and τ_e were performed at 4-6 MPa and 745-916 K, for TRF, B40, B85 and *n*-butanol. Data are summarised in Table 2, along with the important auto-ignition parameters for evaluating ξ-ε plots. The resulting data are plotted in the ξ-ε diagram of Fig. 7.

Table 2. Auto-ignition parameters for stoichiometric mixtures of the different blends at 4-6 MPa, 745-916 K, dT/dr=-2 K and r_0=5 mm.

Thermodynamic condition	Fuel	$10^{-3}\tau_i$ (s)	$10^{-7}\tau_e$ (s)	a (m/s)	$10^{-4}\bar{E}=\tau_i/\tau_e$ $*E/RT$	ξ	ε
P=4 MPa, T=745 K	TRF	4.65	12.21	531.9	3.10	54.10	7.70
	B40	6.73	11.77	533.2	4.96	83.66	7.96
	B85	9.11	10.97	534.8	7.75	122.10	8.52
	n-butanol	9.85	10.62	535.4	8.63	131.74	8.79
P=4 MPa, T=916 K	TRF	2.92	9.53	585.8	2.03	24.78	8.95
	B40	1.59	9.10	587.2	1.24	14.43	9.35
	B85	1.32	8.49	588.9	1.18	12.86	10.01
	n-butanol	1.28	8.24	589.5	1.18	12.50	10.29
P=6 MPa, T=916 K	TRF	1.74	7.71	469.2	1.50	11.83	13.82
	B40	0.96	7.29	587.2	0.93	8.72	11.68
	B85	0.80	6.66	588.9	0.91	7.81	12.75
	n-butanol	0.71	2.25	589.5	0.92	7.58	13.23

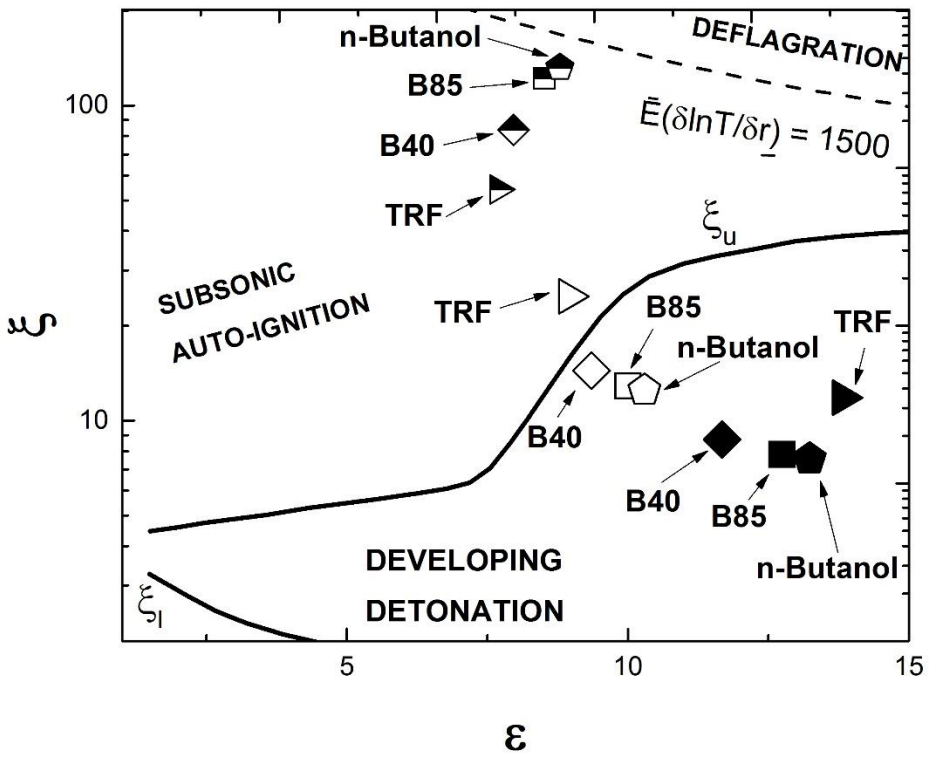

Figure 7. ξ - ε plot for stoichiometric *n*-butanol/TRF blends at higher temperatures and pressures. Symbols: filled 6 MPa and 916 K, open 4 MPa and 916 K, half open 4 MPa and 745 K.

This figure is strikingly different from the earlier Fig. 5. With temperatures of 916 K and pressures of 6 MPa in Fig. 7, there are several points that now lie within the peninsula, with values of ξ < 20, and ε > 10. This is in sharp contrast to Fig. 5, which has lower temperatures of 855 K and pressures of 2 MPa, and no points lying within the peninsula, with all values of ξ > 40 and ε < 12.

In Fig. 7, ξ values were found to decrease with the increase in temperature, whilst values of ε increased. Also, ε values were found to systematically increase with an increase in *n*-butanol concentration at each condition, with an exception of pure TRF at 6 MPa and 916 K. Here, the TRF mixture has the highest ε value of 13.82, compared to any other condition tested. This can be attributed to a substantially lower *a* value of 469.2 m/s.

Consistent with the observations of Gorbatenko et al. [27], *n*-butanol acts as an octane enhancer, increasing τ_i with an increase in its proportion within the blend, at the lower temperature of 745 K. This results in higher ξ values for higher *n*-butanol blends, more remote from the detonation peninsula, and closer to the deflagration regime. Hence, *n*-butanol improves the knock resistance of the blend at 745 K and 4 MPa, although, this is not a regime prone to knock on the ξ/ε diagram.

At 916 K, an increase in the *n*-butanol concentration reduces τ_i and, subsequently, decreases ξ. Here, an addition of *n*-butanol has an opposite effect. The anti-knock resistance of the blend falls with an increase in *n*-butanol concentration, and the blend moves deeper into the detonation development regime. Presently, there is a lack of experimental evidence to evaluate this theoretical finding, i.e. that *n*-butanol enhances the detonation tendency of the resulting blend at high pressures and temperatures. However, it is worth noting that at these temperatures, the dominant reactions controlling the prediction of τ_i and τ_e are those of small molecules whose rates tend to be known with lower uncertainty than fuel specific reactions. Interestingly, at this temperature of 916 K only pure TRF at 4 MPa avoids the bounds of the detonation peninsula.

Reaction pathway analysis has been carried out via the calculation of element fluxes for the H atom. These reveal important pathways for constant volume stoichiometric simulations of B85 and B40 at 916 K and 2 and 6 MPa (flux diagrams are included in Supplementary Information). At higher temperatures, the formation of H_2O_2 is an important pathway for the high concentration *n*-butanol blends (B85). This pathway is found to slightly reduce in its magnitude with pressure, and even more with *n*-butanol concentration (*n*-$C_4H_9OH \rightarrow H_2O_2$: B85 at 6MPa 0.0541, B85 at 2 MPa 0.0525, B40 at 6 MPa 0.0407, B40 at 2 MPa 0.0392). Gorbatenko et al. [27] demonstrated that, at higher temperatures, H abstraction from the α-site of *n*-butanol by HO_2 becomes dominant. This

promotes the reactivity of the system, since this reaction forms H_2O_2. At high temperatures, this subsequently decomposes to form two OH radicals, promoting ignition. The produced OH radicals rapidly consume the fuel at high temperatures, starting a sequence of reactions, in which higher concentrations of OH radicals are formed. The chemistry of H_2O_2 promotes the main stage ignition, inducing the engine knock and detonation. Alternatively, H_2O_2 can react with OH to form H_2O and HO_2, which reduces the reactivity of the system. This channel becomes an increasingly important for lower *n*-butanol concentration blends at the lower pressures. Note, this pathway in not present for B85 at 916 K and 6 MPa in H flux diagram, indicating that it is smaller than the threshold of 0.03. Reaction pathways diagram include only significantly large amounts of H fluxes above this threshold. Also, H abstraction from the α-site of *n*-butanol by HO_2 produces 1-hydroxybutyl, which reacts with oxygen producing *n*-butyraldehyde and HO_2 radical ($C_4H_8OH\text{-}1 + O_2 \leftrightarrow nC_3H_7CHO + HO_2$). This reaction had high sensitivity for B85 at 2 MPa and high temperatures, but it was not featured in case of low *n*-butanol blend (B10) [27]. HO_2 radicals then recombine to form H_2O_2 ($nC_4H_9OH \rightarrow C_4H_8OH\text{-}1 \rightarrow HO_2 \rightarrow H_2O_2$). This alternative pathway has higher production rates of H_2O_2 at 6 MPa compared to 2 MPa. H abstraction from the γ-site by OH also becomes more dominant at higher temperature, leading to a chain branching sequence which promotes auto-ignition [27].

7. Discussion of the Uncertainties and Limitations of the ξ-ε Diagram

Determination of ξ in Eq. (1), requires values of $\frac{\partial T}{\partial r}$ at hot spot centres. These are rarely accurately known, as must also be the value of ξ. Estimating this parameter facilitates comparison of auto-ignition properties of the various fuels to be made. Following Bates at el. [14], a temperature gradient value of $(\partial T/\partial r)$= -2 K/mm was chosen, based on engine and other measurements. On

the other hand, ξ is sensitive to the temperature variation within the hot/cold spot interior, which can affect the value of calculation of ξ.

Simultaneously, providing various physical-chemical properties of fuels, different hot spot magnitudes (r_0= 1 − 12 mm) can be adopted in Eq. (2), where small sizes of hot spots would struggle to sustain the auto-ignition, while the large ones would result in laminar flame propagation, governed by molecular transport [18]. The present study assumes a hot spot radius of 5 mm, which corresponds to turbulent flow length scales and heterogeneities in SI engines, and is consistent with the assumptions made in Bates et al. [39] for CH_4 calculations. In general, within the detonation peninsula framework, omitting a reactivity gradient and mass divergence would prevent a developing detonation from propagating outside the hot spot. However, a developing detonation can occur outside the hot spot and propagate outside the hot spot with damaging consequences [21]. Even more damaging would be strongly developing detonations within numerous hot spots [14, 41], experimentally demonstrated by Pan and Sheppard [42].

The developing detonation regime is bounded by upper and lower limits, ξ_u and ξ_l, the calculations of which have been based on 0.5 H_2 – 0.5 CO fuel, mixed with air, at various equivalence ratios [19]. This regime can be quantitatively very different for the larger hydrocarbon molecule fuels, as has been suggested by Pan et al. [21]. This is a consequence of different physico-chemical properties of fuels that control auto-ignition delay times, diffusion, and transport processes. Detonation development is also strongly controlled by the interplay of pressure waves and heat release. However, the accuracy of excitation times is entirely dependent upon the detailed chemical kinetics, due to the difficulty of experimentally validating short τ_e values. Importantly, uncertainties in the high temperature chemistry of fuels, dominated by small species, have been

shown to be significantly smaller than in the low temperature and NTC regimes, since C_1-C_2 chemistry has been the subject of decades of detailed kinetic studies [43].

Uncertainties and theoretical limitations may cause discrepancies in the detonation peninsula for various fuels, and under various combustion chamber configurations. Nevertheless, despite these uncertainties, the ξ-ε methodology allows differences between fuels to be explored, based on the same fundamental parameterisations. For example, Rudloff et al. [26] and Gorbatenko [44] demonstrated that the elevated knock intensity parameter, π, values are systematically observed for high ε and low ξ values. This implies that these parameters are valuable generalised predictors of knock intensity, despite uncertainties. Further research can help to evaluate the scope of the detonation peninsula for understanding of knocking inhibition.

8. Conclusions

This investigation of the auto-ignition and anti-knock properties of *n*-butanol, TRF and their blends, at 10, 20, 40, and 85% by volume at 2-6 MPa and 678-916 K, has combined RCM measurements and detailed chemical kinetic modelling. The auto-ignition conditions in the RCM or computation, enabled values of ξ and ε to be evaluated. Their location on the on the ξ/ε diagram, relative to the explosion peninsula, enabled their mode of reaction propagation to be predicted. In particular, the severity of any detonation could be assessed, through their location on the ξ/ε diagram, relative to the detonation peninsula.

Different propagation modes are featured on the ξ/ε diagram, including subsonic auto-ignition, deflagration, detonation, and thermal explosion. These arise from the combined effects of spatial and thermodynamic inhomogeneities induced by pressure waves. In RCMs, these inhomogeneities

are more likely to occur with larger values of τ_i, where some deflagrative flame propagation might impair the reliability of measurements. Such conditions are linked to high values of $\bar{E}(\delta lnT/\delta \bar{r})$. It has been shown that, in the RCM, *n*-butanol and its high blends with a gasoline surrogate are on the verge of being affected by hot spot initiation, followed by a small degree of deflagration, indicated by high values of the $\bar{E}(\delta \mathrm{lnT}/\delta \bar{r})$ parameter. On the other hand, the lower *n*-butanol blends and pure TRF clearly lay in the auto-ignition region. This suggests that an RCM is an appropriate facility for ignition delay studies of gasoline-type fuels, provided that these possible limitations are borne in mind.

At 2 MPa and 702– 855 K, all *n*-butanol/TRF blends and their pure components were found to lie outside the bounds of the developing detonation region. The addition of *n*-butanol to the TRF shifted fuels towards the deflagrative/auto-ignitive transition region in the detonation diagram. At blend ratios of 85% *n*-butanol, mixtures were found to lie close to the compression curve of CH_4, which is known to have good anti-knock properties. This implies that an addition of *n*-butanol to gasoline would result in improved anti-knock performance of the blend in practical engine technologies at these temperatures and pressures. In contrast, at 916 K and 6 MPa, the addition of *n*-butanol had the opposite effect, reducing the anti-knock resistance of the blend and moving it deeper into the detonation development region in Fig. 7. This implies that lower *n*-butanol blends are to be preferred for SI engine operations under turbo-charged conditions. Here, the high *n*-butanol blends could potentially lead to detonations and super-knock in gasoline engines, although this requires further exploration.

At 2 MPa and at high temperatures τ_e values fall on the same curve with respect to temperature, regardless of fuel composition, suggesting a limited influence of fuel blend composition on the

main high temperature heat release. There was no apparent effect of *n*-butanol addition to TRF blends, nor any obvious influence from NTC chemistry. Brute force sensitivity analyses for τ_e showed that hydrogen, carbon monoxide, and the smaller C_1 molecule chemistry are dominant in determining the extent of the main heat release. $CO + OH => CO_2 + H$ and $H + O_2 => O + OH$ were found to dominate sensitivity analyses for τ_e for pure TRF and *n*-butanol fuels and their blends. It is suggested that fuel specific reactions affecting low temperature heat release have an indirect influence on the τ_e magnitude, resulting in differences in the duration of the heat release event between different fuel blends at low temperatures.

Finally, despite the inherent uncertainties of ξ and ε, the detonation peninsula framework enables the assessment of the relative differences between the different fuels to be made based on the same fundamental parameterisations.

Acknowledgments

The authors gratefully acknowledge financial support from EPSRC (EP/L01615X/1), regulated by the University of Leeds Centre for Doctoral Training in Fluid Dynamics, as well as Shell Global

Solutions for funding this research. We appreciate helpful discussions with Prof. Roger Cracknell at Shell Global Solutions UK and Dr. Malcolm Lawes at the University of Leeds.

Supplementary Material

TableS1: Auto-ignition parameters for stoichiometric mixtures of the different blends at 2 MPa, dT/dr=-2 K and r_0=5 mm.

T (K)	Fuel	a (m/s)	$10^{-4}\bar{E}=\tau_i/\tau_e$ *E/RT	ξ	ε
702	TRF	460.0	0.92	113.06	1.17
	B10	461.4	1.27	152.33	1.21
	B20	461.9	2.22	262.84	1.22
	B40	467.3	4.30	462.71	1.32
	B85	469.2	2.16	772.48	0.40
	n-butanol	469.0	1.76	640.55	0.40
727	TRF	517.4	3.25	99.19	4.56
	B10	516.8	3.74	115.47	4.51
	B20	517.8	5.29	158.33	4.66
	B40	520.0	15.67	452.87	4.82
	B85	525.0	24.77	648.35	5.30
	n-butanol	527.6	20.28	523.64	5.36
745	TRF	529.6	2.83	72.70	5.28
	B10	527.5	3.41	89.82	5.19
	B20	527.8	4.55	118.31	5.26
	B40	529.5	12.84	328.42	5.33
	B85	532.2	18.38	444.46	5.61
	n-butanol	532.5	12.39	329.42	5.11
765	TRF	533.4	2.69	68.69	5.22
	B10	534.6	4.40	111.32	5.25
	B20	534.9	3.86	95.48	5.37
	B40	537.2	10.71	259.75	5.45
	B85	538.4	19.00	446.23	5.63
	n-butanol	538.8	9.83	236.00	5.52
782	TRF	540.5	2.25	55.47	5.27
	B10	540.9	4.33	105.91	5.30
	B20	541.2	3.37	81.07	5.40
	B40	541.4	9.64	230.48	5.43
	B85	543.9	13.66	309.39	5.71

T (K)	Fuel	a (m/s)	$10^{-4}\bar{E}=\tau_i/\tau_e$ *E/RT	ξ	ε
	n-butanol	545.2	9.07	206.68	5.67
809	TRF	538.5	2.80	57.80	6.16
	B10	542.7	5.02	102.17	6.17
	B20	542.2	3.61	72.21	6.29
	B40	542.0	8.62	166.47	6.51
	B85	543.8	12.45	204.59	7.57
	n-butanol	543.6	7.57	121.03	7.77
831	TRF	542.6	4.50	72.68	7.53
	B10	540.8	6.61	110.11	7.36
	B20	540.8	3.96	63.93	7.61
	B40	541.7	9.39	143.88	7.97
	B85	542.5	9.85	132.16	9.05
	n-butanol	543.8	6.94	87.38	9.60
855	TRF	543.7	3.31	43.09	9.06
	B10	542.0	6.78	91.09	8.85
	B20	542.0	4.39	59.07	8.85
	B40	541.8	10.36	130.15	9.46
	B85	543.4	10.44	112.05	10.99
	n-butanol	543.3	7.23	75.20	11.34

References

[1] European Commission, Climate change consequences, (2019). Available: https://ec.europa.eu/clima/change/consequences_en (accessed 26 August 2019).
[2] European Commission, Renewable energy: Progress reports, (2019). Available: https://ec.europa.eu/energy/en/topics/renewable-energy/progress-reports (accessed 27 August 2019).
[3] X. Gu, Z. Huang, Q. Li, C. Tang, Measurements of laminar burning velocities and Markstein lengths of n-butanol− air premixed mixtures at elevated temperatures and pressures, Energy Fuels 23 (2009) 4900-4907.
[4] B. R. Wigg. A study on the emissions of butanol using a spark ignition engine and their reduction using electrostatically assisted injection. MSc. Thesis, University of Illinois, 2011.
[5] K. Brekke, Butanol an energy alternative, Ethanol Today, (2007) 36-39.
[6] M. Wu, M. Wang, J. Liu, H. Huo, Life-cycle assessment of corn-based butanol as a potential transportation fuel, Argonne National Laboratory: 2007.
[7] G. T. Tsao, A novel 4A process ready for commercial production of ethanol, butanol and hydrogen from cellulosics, Biofuels Symposium, Stewart Center, Purdue University, West Lafayette, Indiana (2008).
[8] N. R. Baral, A. Shah, Techno-economic analysis of cellulosic butanol production from corn stover through acetone–butanol–ethanol fermentation, Energy Fuels 30 (2016) 5779-5790.
[9] G. Kalghatgi, Developments in internal combustion engines and implications for combustion science and future transport fuels, Proc. Combust. Inst. 35 (2015) 101-115.

[10] Z. Wang, H. Liu, R. D. Reitz, Knocking combustion in spark-ignition engines, Progr. Energy Combust. Sci. 61 (2017) 78-112.
[11] D. Bradley, R. Head, Engine autoignition: The relationship between octane numbers and autoignition delay times, Combust. Flame 147 (2006) 171-184.
[12] E. Agbro, A. S. Tomlin, M. Lawes, S. Park, S. M. Sarathy, The influence of n-butanol blending on the ignition delay times of gasoline and its surrogate at high pressures, Fuel 187 (2017) 211-219.
[13] X. Gu, D. Emerson, D. Bradley, Modes of reaction front propagation from hot spots, Combust. Flame 133 (2003) 63-74.
[14] L. Bates, D. Bradley, G. Paczko, N. Peters, Engine hot spots: Modes of auto-ignition and reaction propagation, Combust. Flame 166 (2016) 80-85.
[15] J. Griffiths, J. MacNamara, C. Sheppard, D. Turton, B. Whitaker, The relationship of knock during controlled autoignition to temperature inhomogeneities and fuel reactivity, Fuel 81 (2002) 2219-2225.
[16] J. F. Griffiths, B. Whitaker, Thermokinetic interactions leading to knock during homogeneous charge compression ignition, Combust. Flame 131 (2002) 386-399.
[17] A. B. Mansfield, M. S. Wooldridge, High-pressure low-temperature ignition behavior of syngas mixtures, Combust. Flame 161 (2014) 2242-2251.
[18] L. Bates, D. Bradley, Deflagrative, auto-ignitive, and detonative propagation regimes in engines, Combust. Flame 175 (2017) 118-122.
[19] D. Bradley, C. Morley, X. Gu, D. Emerson, Amplified pressure waves during autoignition: relevance to CAI engines, SAE paper 2002-01-2868, SAE (2002).
[20] N. Peters, G. Paczko, H. Pitsch, Wall Film Evaporation causing Pre-ignition in Turbocharged Gasoline Engines, 25th International Colloquium on the Dynamics of Explosions and Reactive Systems Leeds, UK (2015).
[21] J. Pan, S. Dong, H. Wei, T. Li, G. Shu, L. Zhou, Temperature gradient induced detonation development inside and outside a hotspot for different fuels, Combust. Flame 205 (2019) 269-277.
[22] C. Netzer, L. Seidel, F. Ravet, F. Mauss, Assessment of the validity of RANS knock prediction using the resonance theory, Int. J. Eng. Res. 21 (2020) 610-621.
[23] A. Robert, S. Richard, O. Colin, T. Poinsot, LES study of deflagration to detonation mechanisms in a downsized spark ignition engine, Combust. Flame 162 (2015) 2788-2807.
[24] K. Tanoue, T. Jimoto, T. Kimura, M. Yamamoto, J. Hashimoto, Effect of initial temperature and fuel properties on knock characteristics in a rapid compression and expansion machine, Proc. Combust. Inst. 36 (2017) 3523-3531.
[25] G. Kalghatgi, D. Bradley, J. Andrae, A. Harrison, The nature of 'superknock'and its origins in SI engines, IMechE conference on internal combustion engines: performance fuel economy and emissions (2009) 8-9.
[26] J. Rudloff, J.-M. Zaccardi, S. Richard, J. M. Anderlohr, Analysis of pre-ignition in highly charged SI engines: Emphasis on the auto-ignition mode, Proc. Combust. Inst. 34 (2013) 2959-2967.
[27] I. Gorbatenko, A. S. Tomlin, M. Lawes, R. F. Cracknell, Experimental and modelling study of the impacts of n-butanol blending on the auto-ignition behaviour of gasoline and its surrogate at low temperatures, Proc. Combust. Inst. 37 (2019) 501-509.
[28] D. Goodwin, Cantera: Object-oriented software for reacting flows, (2005). Available: http://www.cantera.org (accessed 17 October 2019).

[29] S. M. Sarathy, P. Oßwald, N. Hansen, K. Kohse-Höinghaus, Alcohol combustion chemistry, Prog. Energy Combust. Sci. 44 (2014) 40-102.
[30] M. Mehl, W. J. Pitz, C. K. Westbrook, H. J. Curran, Kinetic modeling of gasoline surrogate components and mixtures under engine conditions, Proc. Combust. Inst. 33 (2011) 193-200.
[31] E. Agbro, W. Zhang, A. S. Tomlin, A. Burluka, Experimental Study on the Influence of n-Butanol Blending on the Combustion, Autoignition, and Knock Properties of Gasoline and Its Surrogate in a Spark-Ignition Engine, Energy Fuels 32 (2018) 10052-10064.
[32] A. E. Lutz, R. J. Kee, J. A. Miller, H. A. Dwyer, A. K. Oppenheim, Dynamic effects of autoignition centers for hydrogen and C1, 2-hydrocarbon fuels, Symposium (Int.) on Combustion 22 (1989) 1683-1693.
[33] P. Dai, Z. Chen, X. Gan, Effects of CO2 dilution on autoignition and detonation development induced by hot spot in n-heptane/air mixtures, 27th International Colloquium on the Dynamics of Explosions and Reactive Systems (2019).
[34] C. K. Westbrook, M. Mehl, W. J. Pitz, M. Sjöberg, Chemical kinetics of octane sensitivity in a spark-ignition engine, Combust. Flame 175 (2017) 2-15.
[35] S. S. Goldsborough, J. Santner, D. Kang, A. Fridlyand, T. Rockstroh, M. C. Jespersen, Heat release analysis for rapid compression machines: Challenges and opportunities, Proc. Combust. Inst. 37 (2019) 603-611.
[36] S. M. Sarathy, E.-A. Tingas, E. F. Nasir, A. Detogni, Z. Wang, A. Farooq, H. Im, Three-stage heat release in n-heptane auto-ignition, Proc. Combust. Inst. 37 (2019) 485-492.
[37] F. Battin-Leclerc, F. Buda, M. Fairweather, P. Glaude, J. Griffiths, K. Hughes, R. Porter, A. Tomlin, The Effect of Formal Mechanism Reduction on Simulated Propane Autoignition and a Quantitative Assessment of the Impact of Uncertainties in Parameter Values, Proc. Europ. Combust. Meeting, (2005).
[38] J. Griffiths, Reduced kinetic models and their application to practical combustion systems, Progr. Energy Combust. Sci., 21 (1995) 25-107.
[39] L. Bates, D. Bradley, I. Gorbatenko, A. S. Tomlin, Computation of methane/air ignition delay and excitation times, using comprehensive and reduced chemical mechanisms and their relevance in engine autoignition, Combust. Flame 185 (2017) 105-116.
[40] A. Fridlyand, S. S. Goldsborough, M. Al Rashidi, S. M. Sarathy, M. Mehl, W. J. Pitz, Low temperature autoignition of 5-membered ring naphthenes: Effects of substitution, Combust. Flame 200 (2019) 387-404.
[41] D. Bradley, Autoignitions and detonations in engines and ducts, Philosophical Transactions of the Royal Society A: Mathematical, Physical Eng. Sci. 370 (2012) 689-714.
[42] J. Pan, C. G. W. Sheppard, A theoretical and experimental study of the modes of end gas autoignition leading to knock in SI engines, SAE transactions, (1994) 1925-1947.
[43] E. Hébrard, A. S. Tomlin, R. Bounaceur, F. Battin-Leclerc, Determining predictive uncertainties and global sensitivities for large parameter systems: A case study for n-butane oxidation, Proc. Combust. Inst. 35 (2015) 607-616.
[44] I. Gorbatenko. Auto-ignition and heat release of alternative engine fuels. Ph.D. Thesis, University of Leeds, 2019.